

Sealing of PVD coating defects by Ti-O ALD layers for orthopedic implant applications

Zoran Bobić¹, Lazar Kovačević¹, Miha Čekada², Peter Rodič², Atilla Csik³, Branko Škorić¹, Vladimir Terek¹, Pal Terek¹

¹University of Novi Sad, Faculty of Technical Sciences, Novi Sad, Serbia

²Jožef Stefan Institute, Ljubljana, Slovenia

³Institute for Nuclear Research, Debrecen, Hungary

ABSTRACT

With a goal to assess the efficiency of physical vapor deposition (PVD) coating defect sealing by atomic layer deposition (ALD) layers, we investigated the corrosion resistance of PVD TiN and TiN + ALD Ti-O (amorphous and anatase) layers in Hank's solution. The corrosion experiments were conducted on circular areas with 2 mm radius, employing electrochemical impedance spectroscopy (EIS) and potentiodynamic polarization (PD) measurements. To identify defect types, quantities, and their dimensions, confocal and tactile profilometry were performed before and after the corrosion tests. Results revealed that corrosion resistance of layers is influenced by the quantity of through-thickness "critical" defects. The above-coating height of these defects is approximately half of the coating thickness, and their diameter is proportional to the coating's thickness. With an increase in their quantity the corrosion resistance of a coated system decreases. Scanning electron microscopy (SEM) of the focused ion beam (FIB) milled cross-sections revealed a uniform surface coverage by both ALD layers and effective defect sealing. Therefore, application of ALD layer over the PVD coatings emerges as a highly effective strategy for enhancing their corrosion resistance. Additionally, SEM and atomic force microscopy (AFM) analysis of a hybrid layer with anatase TiO₂ revealed formation of protruding nano-features on the surfaces. Such features have promising effects on the bone-cells activity and increased implant osseointegration.

INTRODUCTION

PVD is a widely used technique for applying thin ceramic coatings that enhance the surface properties of materials, i.e. the corrosion resistance. However, the deposition process is accompanied by the formation of growth defects [1,2], which can significantly impact the corrosion behavior of the coated system [3–5]. In previous studies opposing trends about the effect of density of the growth defects on corrosion protection are reported [3–8]. This can be attributed to the fact that previous investigations did not consider the joint influence of the defect size and their density on corrosion properties.

The deposition of a uniform ALD layer over PVD coatings was demonstrated to have significant potential as a method to overcome the influence of PVD growth defects on corrosion protection [9,10]. The ALD is particularly valued for its ability to create highly uniform layers [9,10] that can effectively seal the pinhole type of defects within the PVD coatings [11,12]. However, the effectiveness of the ALD in sealing the pinholes around protrusions type of defects (i.e. nodular defects) was not thoroughly explored.

In this study, the corrosion properties of PVD TiN coatings, with different density of growth defects, and TiN coating with Ti-O ALD overlayer was evaluated. The first goal was to determine the dependence between the defect size and corrosion properties of TiN coatings. The second goal was to evaluate the effect of growth defects on the sealing with ALD layers deposited on TiN coatings

EXPERIMENTAL METHODS

TiN coatings were deposited on polished EN X2CrNiMo17-12-2 (1.4404) substrates in multiple batches using an industrial electron beam evaporation unit BAI 730 (Balzers) and a laboratory reactive sputtering unit Sputron (Balzers) to obtain coatings with varying densities of PVD growth defects

Table 1. Sample designation.

PVD deposition	ALD deposition		
	Amorphous Ti-O	Anatase Ti-O	Anatase and amorphous Ti-O
TiN (Industrial)	TiN _I -AM	TiN _I -AN	TiN _I -AN+AM
TiN (Laboratory)	TiN _L -AM	TiN _L -AN	TiN _L -AN+AM

The ALD technique was used to deposit thin films of amorphous TiO₂, anatase TiO₂, and a double layer of anatase/amorphous TiO₂ onto substrates previously coated with PVD. For the dual layer deposition, anatase was deposited first, followed by the amorphous layer. Both the amorphous and anatase layers, each with a thickness of 50 nm, were deposited using a TFS 200 (Beneq). The depositions were conducted in

thermal mode, with the amorphous layer deposited at 80 °C and the anatase layer at 200 °C. The reactor pressure was maintained at 1.4 mbar, while the chamber pressure was kept at 6.8 mbar during the process. The ALD cycle involved 300 ms of TiCl₄ exposure, which is followed by a 3-second purge, a 300 ms of water vapor exposure, and another 3-second purge. In Table 1 a sample designation is given.

The surface topography characterization was performed with 3D optical (Axio CSM700, Zeiss, Germany) and tactile (Dektak XT device from Bruker) profilometer. 3D tactile measurements were performed over the area of 2x1 mm, with lateral resolutions of 0.3 μm in the X direction and 2 μm in the Y direction. The changes in nanotopography caused by the deposition of ALD layers were studied on predefined locations using atomic force microscopy (AFM) CPM-di (Veeco). AFM measurements were conducted over the areas of 3x3 μm in contact mode using the following parameters: a resolution of 256x256 pixels, setpoint of 225 nN, and a scan rate of 0.5 Hz. Surface analysis, calculation of surface roughness parameters, and PVD growth defect analysis were conducted using SPIP 6.2.0 (Image Metrology) image analysis software.

A dual-beam FIB-SEM microscope Scientific Scios 2 (Thermo Fisher), equipped with an energy dispersive spectroscopy (EDS) analyzer r, was utilized to examine the thickness, uniformity, and sealing effectiveness of the ALD layers.

Corrosion performance was evaluated using EIS and PD techniques. The measurements were performed one hour after the start of exposure, using a three-electrode cell, with 0.785 cm² of the sample exposed to Hank's solution. Corrosion measurements were performed on four different, non-overlapping areas on each sample. The reference electrode was silver/silver chloride (Ag/AgCl, 0.25 V vs. saturated hydrogen electrode), and a carbon rod was used as the counter electrode. Experiments were conducted at room temperature using a Multi Autolab PGSTAT M204 (Metrohm Autolab) potentiostat/galvanostat, controlled by Nova 2.1 software. Electrochemical impedance spectra were obtained over a frequency range of 10 mHz to 100 kHz using a Frequency Response Analyzer (FRA) module. After the EIS measurements, PD measurements were conducted within a potential range of 200 mV below to 1000 mV above the open circuit potential (OCP). The corrosion current (*i_{corr}*) and corrosion potential (*E_{corr}*) were determined from the Tafel plots.

RESULTS

The results of confocal profilometry measurements conducted on TiN_L and TiN_I are presented in Fig. 1. In comparison to the TiN_L the TiN_I has a greater number of dark spots, which correspond to PVD growth defects.

Results of the AFM measurements before and after the deposition of ALD on TiN_L coatings are displayed in Fig 2. Additionally, in this figure the SEM images of surfaces after the ALD are also shown. The deposition of an amorphous TiO₂ layer did not result in a significant change in surface topography. Deposition of anatase TiO₂ led to the formation of

needle-like or grain-like features on the surface, with relatively smooth areas between these features. In the dual ALD layer, group (TiN_L-AN+AM), the surface is completely covered with grain-like or needle-like features.

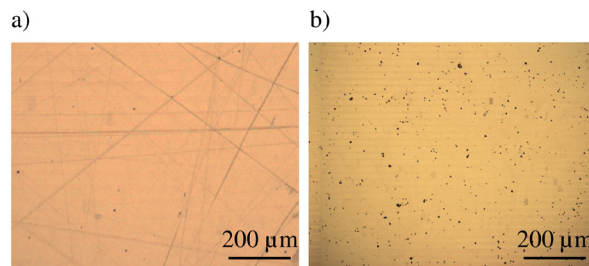


Figure 1. Confocal representative images for a) TiN_L coating and b) TiN_I coating

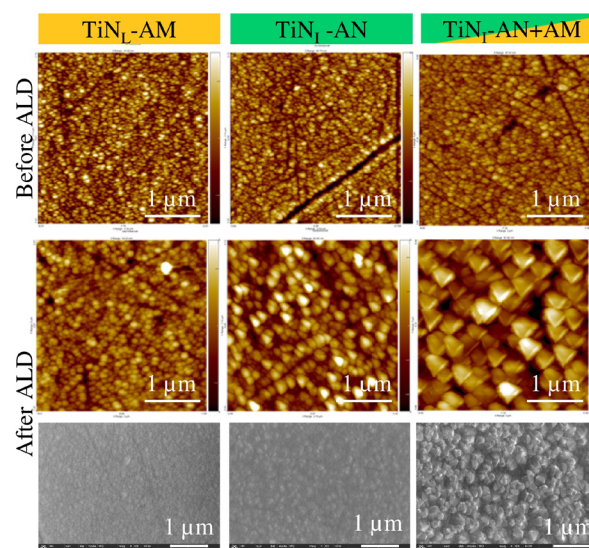


Figure 2. AFM images before and after deposition with SEM images after deposition of examined layers on TiN_I coating.

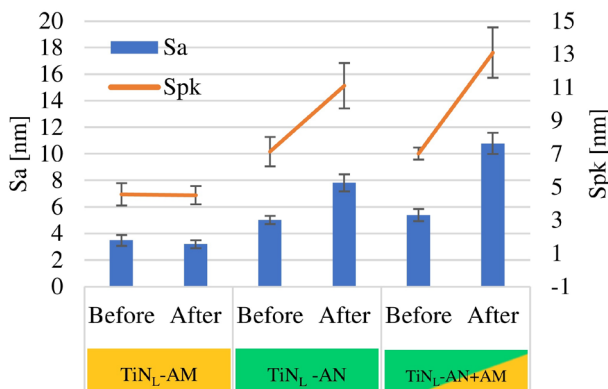


Figure 3. Surface roughness parameters Sa and Spk before and after deposition of ALD layers.

The deposition of amorphous TiO₂(TiN_L-AM) did not significantly affect the surface roughness parameters Sa and

Spk (Fig. 3), unlike the anatase (TiN_L-AN) and dual ALD (TiN_L-AN-AM) TiO₂ layers. However, for TiN_L-AN-AM the changes in these parameters are the most pronounced. Representative SEM images of FIB cross-sections for each ALD layer deposited on TiN_L are shown in Fig. 4. The results demonstrate that the examined ALD layers uniformly cover the surface and no visible defects or cracks near PVD growth defect can be seen.

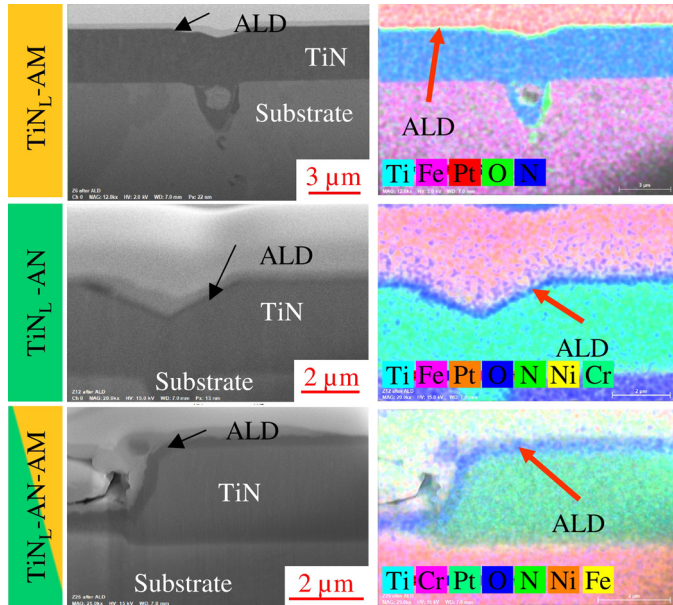


Figure 4. FIB-SEM images of ALD layers cross sections.

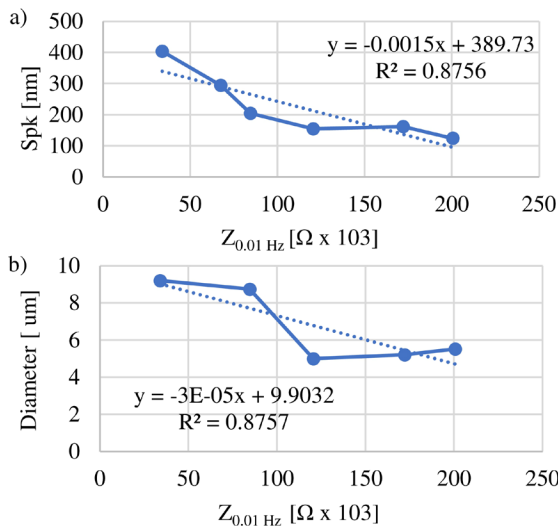


Figure 5. Correlation analysis between $Z_{0.01\text{Hz}}$ and: a) Spk roughness parameter and b) maximal nodular PVD diameter.

The correlation analysis between impedance at 0.01 Hz and the surface roughness parameter Spk, as well as between the impedance and the nodular defects diameter, is presented in Figures 5a and 5b. An increase in the Spk parameter, which

describes the volume of peaks on the observed surface, is associated with a decrease in the impedance. Similarly, an increase in the diameter of the largest nodular defects also leads to a decrease in the impedance. Additionally, there is no significant correlation between the number of nodular defects and impedance.

Figures 6a and 6b display the results of the PD corrosion tests for the TiN_L coating and ALD layers deposited on TiN_L. Compared to TiN_L, the corrosion potential did not change significantly after the ALD deposition. However, there is a pronounced decrease in the corrosion current. The most significant reduction in corrosion current is observed for the TiN_L-AM. Furthermore, the deposition of an amorphous ALD layer on a previously deposited anatase layer (TiN_L-AM-AN) additionally decreased the corrosion current, compared to the TiN_L-AN. However, the corrosion current in the TiN_L-AM-AN remained an order of magnitude lower than that observed for the TiN_L-AM.

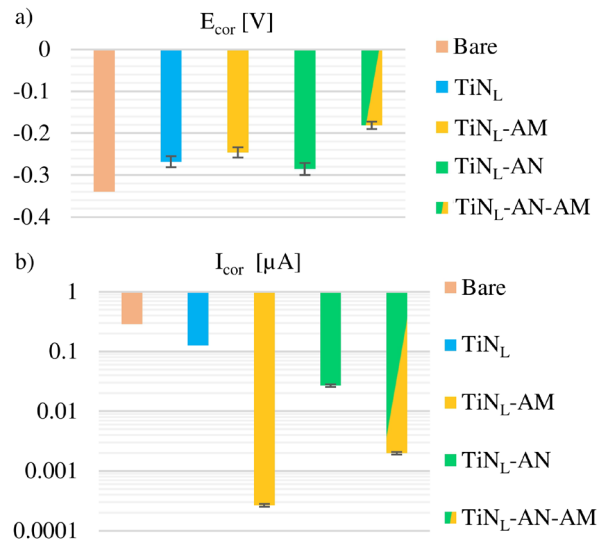


Figure 6. PD results on group with PVD TiN_L coating: a) corrosion potential and b) corrosion current.

Figures 7a and 7b display the results of the PD corrosion tests for the TiN_I coating and ALD layers deposited on TiN_I. The deposition of the TiN_I coating improved the corrosion properties compared to the bare substrate. However, the deposition of either amorphous (TiN_I-AM) or anatase (TiN_I-AN) TiO₂ layers did not provide a notable enhancement in corrosion potential and current. In contrast, dual layer (TiN_I-AN-AM) configuration induced a pronounced improvement in corrosion current.

Figures 8a and 8b present the results of PD corrosion tests conducted on different locations of TiN_I-AM and TiN_I-AN-AM samples. The results revealed a relatively high variation in the corrosion current on the testing location.

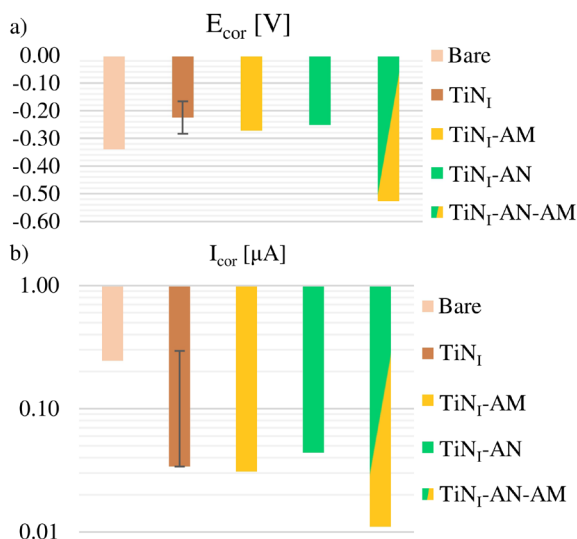


Figure 7. PD results on group with PVD TiN_1 coating: a) corrosion potential and b) corrosion current.

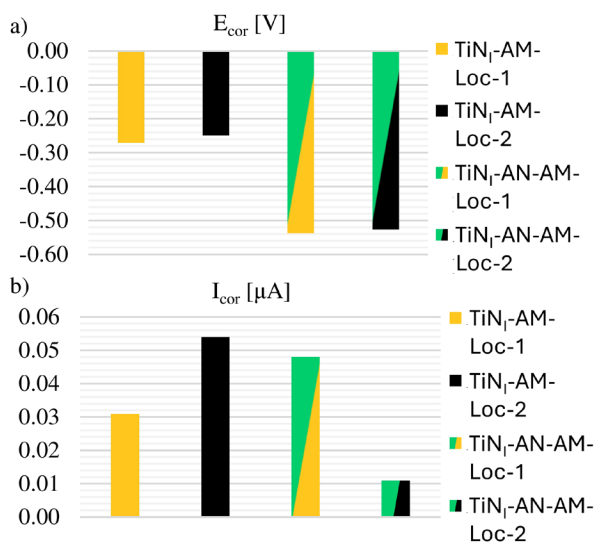


Figure 8. PD results performed on one sample for group TiN_1-AM and $TiN_1-AN-AM$: a) Corrosion potential and b) Corrosion current

DISCUSSION

Previous investigations suggested that an increase in the overall density of defects did not necessarily decrease corrosion resistance [3–5]. Studies [6–8] indicated that the size of defects could determine whether a PVD defect would act as an active site for corrosion process. In other words, researchers in [2–4,13–16] suggested that larger defects and an increase in their density could lead to a more pronounced reduction in corrosion properties.

In this study, samples with TiN coatings deposited in a laboratory unit had a significantly lower density of PVD growth defects than those deposited in an industrial unit (Fig. 1). Since

the substrates were prepared using the same procedure, the probability of defect formation due to geometric factors related to surface topography features [8] was similar in both deposition units. The difference in defect density could be caused by a higher presence of impurities in the industrial chamber during the deposition process [8]. Even though the density of defects is greater for the TiN_L than the TiN_L coating, the corrosion properties are better for TiN_L . This difference is likely to occur due to differences in coating microstructure that could have also affected the corrosion resistance [17]. Correlation analysis revealed that the overall density of PVD defects does not correlate well with changes in the impedance, which is in line with findings from previous investigations [3–5]. Instead, the S_{pk} surface roughness parameter and the diameter of the largest nodular defect showed a strong correlation with changes in the impedance (Fig. 5a and 5b). These findings confirm previous suggestions that the size of defects, rather than the overall density of defects, has a greater influence on corrosion properties [6–8]. However, more comprehensive investigations are needed to confirm these results.

The capability of ALD deposition to produce nearly defect-free, uniform thin films has been well-documented [18–23]. In works [10–12,24–30] the application of thin ALD layers on previously deposited PVD coatings has been extensively examined and it was demonstrated that the deposition of ALD layers significantly improves corrosion properties. This improvement was primarily attributed to the ability of the uniform thin ALD layer to seal pinholes in PVD coatings [12].

The deposition of the examined ALD layers on TiN_L resulted in the formation of a uniform layer (Fig. 4) and led to enhanced corrosion resistance (Fig. 6). This result is consistent with the previous findings [10–12,24–30]. The deposition of anatase layers changed the surface topography due to the formation of TiO_2 crystals, whereas the deposition of the amorphous layer did not cause any changes in it. The presence of these crystals, combined with slightly higher deposition temperatures, could have introduced higher residual stress in the ALD layer of TiN_L-AN group [31]. Consequently, this reduced its effectiveness in sealing the PVD defects in comparisons to amorphous TiO_2 layer of TiN_L-AM group. In the case of the $TiN_L-AN-AM$ group, larger crystals uniformly cover the surface without a visible amorphous matrix around the anatase grains (Fig. 2). This suggests that the ALD deposition parameters used for deposition of the amorphous layer over the previously deposited anatase layer promoted further formation or growth of anatase grains, resulting in an increase in surface roughness (Fig. 2 and 3) and crystallinity. Increased crystallinity [32] and thickness [12] of ALD layer potentially lead to increased corrosion resistance compared with the anatase ALD layer alone.

The deposition of the ALD layer over the TiN_L coating produced in an industrial unit did not significantly improve the corrosion properties (Fig. 7). The most notable improvement is observed for $TiN_L-AN-AM$ group, which could be caused by increased thickness of the ALD layer.

Based on the results (Figs. 6, 7, 8) from this investigation, it is suggested that the efficacy of defect sealing with ALD layers is influenced by density and the dimensional characteristics (i.e. diameter) of PVD growth defects. PVD defects are microlocations where the surface deviates significantly from an ideal flat surface, and it is characterized by abrupt local transitions in surface geometry. These areas are susceptible to stress concentration, which together with the layer residual stresses can lead to crack formation and fracture of the ALD layer. However, further investigation is needed to confirm this finding.

CONCLUSIONS

In this investigation, the corrosion protection of TiN PVD coatings, with and without different ALD Ti-O layers, was evaluated. The study aimed to determine the influence of PVD growth defects on the corrosion protection of these coatings. Additionally, the goal was to assess the effectiveness of the various ALD layers in sealing the PVD growth defects. Based on the presented results, the following conclusions can be drawn:

- The PVD TiN coating improves the corrosion resistance of the underlay substrate.
- While the overall density of PVD growth defects does not correlate with corrosion resistance, the diameter of the largest nodular PVD defect reveals a significant correlation with this property.
- The amorphous TiO₂ ALD layer demonstrates superior sealing effectiveness compared to the anatase TiO₂ layers. It can be postulated that this is due to the higher residual stress present in the anatase TiO₂ layer.
- This is because the defects are the sites with abrupt changes in surface geometry where the ALD layers can crack due to the high stress concentration. Further investigation need to confirm the previous.

REFERENCES

[1] P. Panjan, A. Drnovšek, P. Gselman, M. Čekada, M. Panjan, T. Bončina, D.K. Merl, Influence of growth defects on the corrosion resistance of sputter-deposited TiAlN hard coatings, *Coatings*. 9 (2019) 1–16. <https://doi.org/10.3390/coatings9080511>.

[2] P. Panjan, M. Čekada, M. Panjan, D. Kek-Merl, F. Zupanič, L. Čurković, S. Paskvale, Surface density of growth defects in different PVD hard coatings prepared by sputtering, *Vacuum*. 86 (2012) 794–798. <https://doi.org/10.1016/j.vacuum.2011.07.013>.

[3] D.K. Merl, P. Panjan, M. Panjan, M. Čekada, The role of surface defects density on corrosion resistance of PVD hard coatings, *Plasma Process. Polym.* 4 (2007) 613–617. <https://doi.org/10.1002/ppap.200731416>.

[4] I.M. Penttinen, A.S. Korhonen, E. Harju, M.A. Turkia, O. Forsén, E.O. Ristolainen, Comparison of the corrosion resistance of TiN and (Ti,Al)N coatings, *Surf. Coatings Technol.* 50 (1992) 161–168.

[5] M. Balzer, Identification of the growth defects responsible for pitting corrosion on sputter-coated steel samples by Large Area High Resolution mapping, *Thin Solid Films*. 581 (2015) 99–106. <https://doi.org/10.1016/j.tsf.2014.12.014>.

[6] T. Spalvins, Characterization of defect growth structures in ion-plated films by scanning electron microscopy, *Thin Solid Films*. 64 (1979) 143–148. [https://doi.org/10.1016/0040-6090\(79\)90553-4](https://doi.org/10.1016/0040-6090(79)90553-4).

[7] X. Ling, J. Shao, Z. Fan, Thermal-mechanical modeling of nodular defect embedded within multilayer coatings, *J. Vac. Sci. Technol. A Vacuum, Surfaces, Film*. 27 (2009) 183–186. <https://doi.org/10.1116/1.3065676>.

[8] P. Panjan, A. Drnovšek, P. Gselman, M. Čekada, M. Panjan, Review of growth defects in thin films prepared by PVD techniques, MDPI AG, 2020. <https://doi.org/10.3390/COATINGS10050447>.

[9] J.S. Daubert, G.T. Hill, H.N. Gotsch, A.P. Gremaud, J.S. Ovental, P.S. Williams, C.J. Oldham, G.N. Parsons, Corrosion Protection of Copper Using Al₂O₃, TiO₂, ZnO, HfO₂, and ZrO₂ Atomic Layer Deposition, *ACS Appl. Mater. Interfaces*. 9 (2017) 4192–4201. <https://doi.org/10.1021/acsami.6b13571>.

[10] E. Kaady, A. Alhoussein, M. Bechelany, R. Habchi, Al₂O₃-ZnO atomic layer deposited nanolaminates for improving mechanical and corrosion properties of sputtered CrN coatings, *Thin Solid Films*. 759 (2022) 139476. <https://doi.org/10.1016/j.tsf.2022.139476>.

[11] J. Leppäniemi, P. Sippola, A. Peltonen, J.J. Aromaa, H. Lipsanen, J. Koskinen, Effect of Surface Wear on Corrosion Protection of Steel by CrN Coatings Sealed with Atomic Layer Deposition, *ACS Omega*. 3 (2018) 1791–1800. <https://doi.org/10.1021/acsomega.7b01382>.

[12] E. Härkönen, I. Kolev, B. Díaz, J. Światowska, V. Maurice, A. Seyeux, P. Marcus, M. Fenker, L. Toth, G. Radnoczi, M. Vehkamäki, M. Ritala, Sealing of hard CrN and DLC coatings with atomic layer deposition, *ACS Appl. Mater. Interfaces*. 6 (2014) 1893–1901. <https://doi.org/10.1021/am404906x>.

[13] D.B. Lewis, S.J. Creasey, C. Wüstefeld, A.P. Ehiasarian, P.E. Hovsepian, The role of the growth defects on the corrosion resistance of CrN/NbN superlattice coatings deposited at low temperatures, *Thin Solid Films*. 503 (2006) 143–148. <https://doi.org/10.1016/j.tsf.2005.08.375>.

[14] S.H. Ahn, J.H. Lee, J.G. Kim, J.G. Han, Localized corrosion mechanisms of the multilayered coatings related to growth defects, *Surf. Coatings Technol.* 177–178 (2004) 638–644. [https://doi.org/10.1016/S0257-8972\(03\)00939-3](https://doi.org/10.1016/S0257-8972(03)00939-3).

[15] H. Hoche, C. Pusch, M. Oechsner, Establishing PVD-coatings for the corrosion protection of mild steel substrates for complex tribological and corrosive stresses, *Surf. Coatings Technol.* 376 (2019) 74–83.

- <https://doi.org/10.1016/j.surfcoat.2018.06.007> .
- [16] H.W. Wang, M.M. Stack, S.B. Lyon, P. Hovsepian, W.D. Münz, The corrosion behaviour of macroparticle defects in arc bond-sputtered CrN/NbN superlattice coatings, *Surf. Coatings Technol.* 126 (2000) 279–287. [https://doi.org/10.1016/S0257-8972\(00\)00554-5](https://doi.org/10.1016/S0257-8972(00)00554-5) .
- [17] J.L. Daure, K.T. Voisey, P.H. Shipway, D.A. Stewart, The effect of coating architecture and defects on the corrosion behaviour of a PVD multilayer Inconel 625/Cr coating, *Surf. Coatings Technol.* 324 (2017) 403–412. <https://doi.org/10.1016/j.surfcoat.2017.06.009> .
- [18] J.S. Daubert, G.T. Hill, H.N. Gotsch, A.P. Gremaud, J.S. Ovental, P.S. Williams, C.J. Oldham, G.N. Parsons, Corrosion protection of copper using Al₂O₃, TiO₂, ZnO, HfO₂, and ZrO₂ Atomic layer deposition, *ACS Appl. Mater. Interfaces.* 9 (2017) 4192–4201. <https://doi.org/10.1021/acsami.6b13571> .
- [19] I. Spajić, E. Rahimi, M. Lekka, R. Offoiach, L. Fedrizzi, I. Milošev, Al₂O₃ and HfO₂ Atomic Layers Deposited in Single and Multilayer Configurations on Titanium and on Stainless Steel for Biomedical Applications, *J. Electrochem. Soc.* 168 (2021) 071510. <https://doi.org/10.1149/1945-7111/ac131b> .
- [20] F. Bilo, L. Borgese, J. Prost, M. Rauwolf, A. Turyanskaya, P. Wobruschek, P. Kregsamer, C. Strelj, U. Pazzaglia, L.E. Depero, Atomic layer deposition to prevent metal transfer from implants: An X-ray fluorescence study, *Appl. Surf. Sci.* 359 (2015) 215–220. <https://doi.org/10.1016/j.apsusc.2015.09.248> .
- [21] E.C.S. Transactions, T.E. Society, L. Borgese, F. Bilo, A. Zacco, E. Bontempi, M. Pasquali, S. Federici, J. Prost, M. Rauwolf, A. Turyanskaya, C. Strelj, P. Kregsamer, P. Wobruschek, L.E. Depero, ALD to prevent metal transfer from implants L. Borgese, *ECS Trans.* 75 (2016) 167–175. <https://doi.org/10.1149/07506.0167ecst> .
- [22] H.C. Lin, Y.L. Chang, Y.Y. Han, K.C. Yang, M.C. Chen, Atomic layer deposited Al₂O₃ films on NiTi shape memory alloys for biomedical applications, *Procedia Manuf.* 37 (2019) 431–437. <https://doi.org/10.1016/j.promfg.2019.12.070> .
- [23] S. Hashemi Astanah, L.P. Faverani, C. Sukotjo, C.G. Takoudis, Atomic layer deposition on dental materials: Processing conditions and surface functionalization to improve physical, chemical, and clinical properties - A review, *Acta Biomater.* 121 (2021) 103–118. <https://doi.org/10.1016/j.actbio.2020.11.024> .
- [24] E. Marin, L. Guzman, A. Lanzutti, L. Fedrizzi, M. Saikkonen, Chemical and electrochemical characterization of hybrid PVD + ALD hard coatings on tool steel, *Electrochem. Commun.* 11 (2009) 2060–2063. <https://doi.org/10.1016/j.elecom.2009.08.052> .
- [25] W. Dai, Q. Wang, K.H. Kim, S.H. Kwon, Al₂O₃/CrAlSiN multilayer coating deposited using hybrid magnetron sputtering and atomic layer deposition, *Ceram. Int.* 45 (2019) 11335–11341. <https://doi.org/10.1016/j.ceramint.2019.02.211> .
- [26] J. Leppäniemi, P. Sippola, M. Broas, J. Aromaa, H. Lipsanen, J. Koskinen, Corrosion protection of steel with multilayer coatings: Improving the sealing properties of physical vapor deposition CrN coatings with Al₂O₃/TiO₂ atomic layer deposition nanolaminates, *Thin Solid Films.* 627 (2017) 59–68. <https://doi.org/10.1016/j.tsf.2017.02.050> .
- [27] C.X. Shan, X. Hou, K. Choy, P. Choquet, Improvement in corrosion resistance of CrN coated stainless steel by conformal TiO₂ deposition, *202 (2008) 2147–2151.* <https://doi.org/10.1016/j.surfcoat.2007.08.078> .
- [28] M. Staszuk, D. Pakuła, Ł. Reimann, A. Kloc-Ptaszna, M. Pawlyta, A. Kříž, Structure and properties of TiO₂/nanoTiO₂ bimodal coatings obtained by a hybrid PVD/ALD method on 316L steel substrate, *Materials (Basel).* 14 (2021). <https://doi.org/10.3390/ma14164369> .
- [29] J.H. Min, Y.A. Chen, I. Te Chen, T. Sun, D.T. Lee, C. Li, Y. Zhu, B.T. O’Connor, G.N. Parsons, C.H. Chang, Conformal Physical Vapor Deposition Assisted by Atomic Layer Deposition and Its Application for Stretchable Conductors, *Adv. Mater. Interfaces.* 5 (2018). <https://doi.org/10.1002/admi.201801379> .
- [30] Wan, T.F. Zhang, J.C. Ding, C.M. Kim, S.W. Park, Y. Yang, K.H. Kim, S.H. Kwon, Enhanced Corrosion Resistance of PVD-CrN Coatings by ALD Sealing Layers, *Nanoscale Res. Lett.* 12 (2017) 1–8. <https://doi.org/10.1186/s11671-017-2020-1> .
- [31] O.M.E. Ylivaara, A. Langner, X. Liu, D. Schneider, J. Julin, K. Arstila, S. Sintonen, S. Ali, H. Lipsanen, T. Sajavaara, S.P. Hannula, R.L. Puurunen, Mechanical and optical properties of as-grown and thermally annealed titanium dioxide from titanium tetrachloride and water by atomic layer deposition, *Thin Solid Films.* 732 (2021). <https://doi.org/10.1016/j.tsf.2021.138758> .
- [32] D. Tromans, Thermodynamic Evaluation of the Effects of Amorphism on Film Breakdown and Pitting Initiation, *J. Electrochem. Soc.* 152 (2005) B460. <https://doi.org/10.1149/1.2048169> .

FOR FURTHER INFORMATION

Zoran Bobic - University of Novi Sad, Faculty of Technical Sciences, Novi Sad, Serbia. E-mail: zoranbobic@uns.ac